Size, temperature, and bond nature dependence of elasticity and its derivatives on extensibility, Debye temperature, and heat capacity of nanostructures

M. X. Gu,[1] Chang Q. Sun,[1,*] Z. Chen,[2] T. C. Au Yeung,[1] S. Li,[3] C. M. Tan,[1] and V. Nosik[4]
[1]*School of Electronic and Electrical Engineering, Nanyang Technological University of Singapore, 639798, Singapore*
[2]*School of Materials Science and Engineering, Nanyang Technological University of Singapore, 639798, Singapore*
[3]*School of Materials Science, The University of New South Wales, NSW 2052, Australia*
[4]*ST Microelectronics, 10 Science Park Road, #02-08, The ALPHA, Singapore Science park II, 117684, Singapore*
(Received 22 May 2006; revised manuscript received 24 November 2006; published 2 March 2007)

With the miniaturization of a solid down to nanometer scale, the elasticity, extensibility, Debye temperature, and specific heat capacity of the solid are no longer constant but change with variation of size. These quantities also change with the temperature of the measurement and the nature of the chemical bond involved. The mechanism behind the intriguing tunability and the interdependence of these quantities remain yet a high challenge. A set of analytical solutions is presented herewith showing that the observed trends could be reproduced by taking the fact of bond order deficiency into consideration. Agreement between predictions and observations clarifies that the shortened and strengthened surface bonds dictate intrinsically the observed tunability, yet atoms in the core interior remain as they are in the bulk. The thermally softening of a specimen arises from bond expansion and bond vibration due to the internal energy increases.

DOI: 10.1103/PhysRevB.75.125403 PACS number(s): 61.46.−w, 62.25.+g, 65.40.−b

I. INTRODUCTION

Young's modulus (Y) is one of the key elemental parameters in materials science, which is related to the performance of a material such as the elasticity, extensibility, acoustic transmission velocity, Debye temperature, specific heat capacity, and thermal conductivity of the specimen. Traditionally, the Young's modulus in a bulk material is deemed as constant at a given temperature[1] and the value of the modulus is proportional to the melting point (T_m) of the bulk. However, upon structural miniaturization to the nanometer regime, the Young's modulus is no longer constant but changes with the shape and size of the solid. Measurements have revealed surprisingly that the Y value changes in three different ways: elevation, depression, or retention as the solid size is reduced. For inorganic nanomaterials with higher T_m, the modulus is often measured to increase at the ambient temperature when the solid size is decreased, such as observed from Si nanospheres,[2] Ag nanowires,[3] quartz crystal oscillators,[4] Si_3N_4 nanobelts,[5] TiCrN and TiAlN surfaces,[6] Al and Si nanobelts,[7] ZnO nanowires,[8] and nanobelts.[9] However, an opposite trend is presented in (0001)-oriented ZnO nanobelts and wires showing lower modulus varying from 29±8 (Ref. 10) to 38–100 GPa (Refs. 11 and 12) compared with that of the bulk ZnO obtainel at 140 GPa. An atomic force acoustic microscopy (AFAM) measurement[13] has revealed that the modulus of nanocrystallined Ni films of 50–800 nm thick is lower than the bulk value. An atomic force microscopy (AFM) room temperature measurement[14] has revealed that the local Young's modulus of organic thin films that can evaporate at ~450 K decreases with sizes. The moduli of Cr (Ref. 15) and Sr (Ref. 16) nanocantilevers and ZnS (Ref. 17) nanobelts are also measured to decrease sharply with decreasing diameters. In contrast, amorphous Si nanowires,[18] Au (Ref. 19) and Ag (Ref. 20) nanowires show no apparent change with size despite the scattered error bars in the measurement. Therefore, it appears quite confusing that even for the same materials such as Ni, Ag, ZnO, and Si, the Y value changes in different ways, depending on the experimental techniques and operation conditions.

On the other hand, the modulus or strength, being correlated linearly, of a solid generally drops associated with enhancement of extensibility when the testing temperatures are raised,[21] such as the cases of nanograined Al (Ref. 22) and diamond films.[23] At higher temperatures the bending stiffness and the apparent Young's modulus of the diamond beams are drastically reduced to one-third of the initial value before fracture. The flexural strength and modulus of hydrosilylation and condensation reaction curable silicone resins also decrease when the testing temperatures are raised.[24]

The elastic response of nanostructures has been theoretically attributed to nonlinear effects,[25] surface reconstruction,[26] surface stress,[27,28] and surface strain.[6,8,29] However, an atomistic understanding of the size, temperature, and bond nature dependence of the modulus of a solid and its derivatives on the extensibility, Debye temperature, and heat capacity is yet lacking though a recent molecular dynamics simulation[30] suggests that surface atoms play an important yet unclear role in the mechanical behaviors of nanostructures. An analytical expression for the size, temperature, and bond nature dependence of the intrinsic mechanical properties of nanomaterials is therefore highly desirable. Here we show that an extension of the recently developed bond-order-length-strength (BOLS) correlation mechanism[31–33] to temperature domain could reproduce the observed trends and hence clarify for the first time the long-standing discrepancy in observations.

II. PRINCIPLES

A. Broken bond and BOLS correlation

The core idea of the BOLS correlation[31,32] is that broken bonds of surface atoms make the remaining bonds (with

length d_i and bond energy E_i) between the undercoordinated atoms shorter, $d_i=c_i d$, and stronger, $E_i=c_i^{-m}E_b$ with respect to the bulk counterparts, where $c_i(z_i)=2\{1+\exp[(12-z_i)/(8z_i)]\}^{-1}$ is the coefficient of bond contraction with z_i being the effective coordination of the specific ith atomic layer of concern (where $i=1$ for outermost layer). The superscript m is a bond nature indicator. The binding energy per bond is given approximately as $E_b=\eta_1 T_m+\eta_2$ with η_1 the specific heat per bond and η_2 the $1/z_b$ fold of latent heat for atomization of the atom in molten state. The specific heat η_1 follows the universal Debye relation of temperature dependence. As a result of a bond broken, localized densification of charge, mass, and energy occurs to the surface skin, which perturbs the Hamiltonian, atomic coherency (the product of single bond energy and the number of bond of a specific atom), and electroaffinity (separation between vacuum level and the conduction band edge) and associated properties of a specimen with considerable portion of the undercoordinated atoms, in particular. The competition between the atomic coherency (determines the melting point) and energy densification (mechanical strength) in the surface skin dictates the elastic modulus, stress, and extensibility of the entire solid. The bond-strengthening-induced depression of the potential well of trapping will affect the transport dynamics of phonons, electrons, and photons.

B. *T*-dependent Young's modulus and extensibility

1. Temperature dependence

Taking temperature into consideration, the local stress P_i and the Young's modulus Y_i at the specific ith atomic site at a given temperature can be expressed as[34]

$$\left.\begin{aligned} P_i(z_i,m,T) &= -\left.\frac{\partial u(r,m,T)}{\partial V}\right|_{d_i} \\ Y_i(z_i,m,T) &= -V\left.\frac{\partial P(z_i,m,T)}{\partial V}\right|_{d_i} \end{aligned}\right\} \propto E_i(z,T)/d_i^3(z,T), \quad (1)$$

where $u(r,m,T)$ is the interatomic pairing potential and V the volume. The $d(z_i,T)$ and $E_i(z_i,T)$ correspond to the coordination- and temperature-dependent bond length and the net bond energy:

$$d_i(z_i,T)=d_0c_i\left(1+\int_0^T \alpha_i(t)dt\right) \cong d_0c_i(1+\alpha_i T) \overset{\alpha T\ll 1}{\approx} d_0c_i,$$

$$E_i(z_i,T)=E_bc_i^{-m}-\int_0^T \eta_{1i}(t)dt \overset{T\gg\theta_D}{\cong} c_i^{-m}E_b-\eta_{1i}T$$

$$=\eta_{2i}+\eta_{1i}(T_{mi}-T), \quad (2)$$

with $\alpha_i(t)$ being the temperature-dependent thermal expansion coefficient. T_{mi} is the local melting point. The η_{1i} remains constant at temperatures that are higher than the Debye temperature. Therefore, Eq. (1) can be expressed as

$$\left.\begin{aligned} &P_i(z_i,m,T) \\ &Y_i(z_i,m,T) \end{aligned}\right\} \propto \begin{cases} \dfrac{\int_T^{T_{mi}}\eta_{1i}(t)dt}{d_i(1+\alpha_i T)^3} \overset{T\gg\theta_D}{=} \dfrac{\eta_{1i}(T_{mi}-T)}{d_i(1+\alpha_i T)^3} & \text{(Born)}, \\ \dfrac{\eta_{2i}+\int_T^{T_{mi}}\eta_{1i}(t)dt}{d_i(1+\alpha_i T)^3} \overset{T\gg\theta_D}{=} \dfrac{\eta_{2i}+\eta_{1i}(T_{mi}-T)}{d_i(1+\alpha_i T)^3} & \text{(BOLS)}. \end{cases}$$

According to Born's criterion[35] of melting, the modulus disappears when a solid is at melting. Measurements[36,37] also reveled that the tensile strength of alloys drops from the bulk values to approximately zero when the temperature approaches T_m. If Born's criterion holds in effect, the latent heat of atomization makes no contribution to the mechanical strength. However, an elastic modulus should present in liquid and gases phases as the nonzero sound velocity in these phases. Therefore, Born's criterion may be taken as a crude approximation in modeling consideration. For modeling convenience, we may define a cutoff temperature at which the mechanical strength approaches zero. Precisely, the Y and P are the derivatives of interatomic potential $u(r,m,T)$. However, there exists uncertainty in choosing the exact form of the $u(r,m,T)$ and what we are concerned with is the relative change of Y and P to the bulk values. On the other hand, from the analysis of dimension, the P and Y are both proportional to the energy per unit volume. Therefore, it is reasonable to take the above approximation in the analytical modeling. It is unnecessary and impractical to consider the differentiations at a point of distance away from the equilibrium atomic distance. An exact solution may be obtained in the first-principles calculations but the outcome will also be subject to the $u(r,m,T)$ selected.

An analytical solution for thermal depression of the Young's modulus has long been a challenge in particular in terms of atomic bonding.[38] Wachtman *et al.*[39,40] proposed a empirical expression for T-dependent Young's modulus and later Anderson[41] proposed an expression for the T dependence from the perspective of anharmonic lattice vibration, which are compared with the current proposal for large chunks ($c_i=1$) as follows:

$$\frac{\Delta Y(T)}{Y_0}=\begin{cases} -AT\exp(-T_0/T)\approx A(T_0-T) & \text{(Wachtman)}, \\ -BT\times F(T/\theta_D)=-BU(T) & \text{(Anderson)}, \\ \dfrac{1}{(1+\alpha_i T)^3}\left(1-\dfrac{\int_0^T\eta_1(t)dt}{E_b(0)}\right)-1\approx\dfrac{E_b(0)-\eta_1 T}{(1+\alpha_i T)^3E_b(0)}-1 \overset{\alpha T\ll 1}{\sim} -[E_b(0)]^{-1}U(T) & \text{(BOLS)}, \end{cases}$$

where A, B, and T_0 are adjustable. $\eta_1(t)$ is the Debye specific heat, and

$$U(T) = TF(T/\theta_D) = 3\theta_D\left(\frac{T}{\theta_D}\right)^4 \int_0^{\theta_D/T} \frac{x^3\,dx}{e^x - 1} = \int_0^{\theta_D/T} \eta_1(t)dt \sim \eta_1 T$$

is the internal energy, being the integration of $\eta_1(t)$.

2. Size dependence

Considering the fact that the T_{mi} is proportional to atomic cohesive energy,[31] $T_{mi} \propto z_i E_i$, we have the relation $T_{mi}/T_m = z_i E_i / z_b E_b = z_{ib} c_i^{-m} = 1 + \Delta_i$ with Δ_i being the perturbation to the atomic coherency. $z_{ib} = z_i / z_b$ is the normalized atomic coordination with $z_b = 12$ being the standard value in fully coordinated system.[42] With the relation of $E_i = c_i^{-m} E_b = \eta_{1i} T_{mi} + \eta_{2i} = c_i^{-m}$ $(\eta_1 T_m + \eta_2)$ and $T_{mi} = z_{ib} c_i^{-m} T_m = (1 + \Delta_i) T_m$, we have $\eta_{1i} = z_{bi}\eta_1$ and $\eta_{2i} = c_i^{-m}\eta_2$ The relative change of the local Y and its inverse, or the extensibility β, of a solid measured at $T \gg \theta_D$ can be simplified,

$$\delta_Y(m, z_i, T) = \frac{Y(m, z_i, T)}{Y(m, z_b, T_0)} - 1 = c_i^{-(3+m)+m}\frac{\eta_{1i}(T_{mi} - T) + \eta_{2i}}{\eta_1(T_m - T_0) + \eta_2} - 1 = c_i^{-(3+m)}\left(\frac{T_m - T/(1+\Delta_i) + \eta_{21}}{T_m - T_0 + \eta_{21}}\right) - 1 = c_i^{-(3+m)}\left(1 + \frac{T_0 - T/(1+\Delta_i)}{T_m - T_0 + \eta_{21}}\right) - 1,$$

$$\delta_\beta(m, z_i, T) = \frac{\beta(m, z_i, T)}{\beta(m, z_b, T_0)} - 1 = c_i^{(3+m)}\frac{T_m - T_0 + \eta_{21}}{T_{mi} - T/(1+\Delta_i) + \eta_{21}} - 1 = c_i^{(3+m)}\left(1 - \frac{T_0 - T/(1+\Delta_i)}{T_m - T/(1+\Delta_i) + \eta_{21}}\right) - 1.$$

Taking the core-shell configuration of a nanosolid into consideration, the bond nature (m), shape and size (τ, K_j), and temperature (T) dependence of the relative change of the Y can be obtained by summing contribution over the outermost three atomic layers:

$$\frac{\Delta Y(m, K_j, T)}{Y(m, \infty, T_0)} = \sum_{i \leqslant 3} \gamma_{ij}\delta_Y(m, z_i, T)$$

$$\delta_Y(m, z_i, T) = \begin{cases} c_i^{-(3+m)}\left(1 + \dfrac{T_0 - T/(1+\Delta_i)}{T_m - T_0 + \eta_{21}}\right) - 1 & (T \neq T_0; K_j \neq \infty), \\ \dfrac{T_0 - T}{T_m - T_0 + \eta_{21}} & (T \neq T_0; K_j = \infty), \\ c_i^{-(3+m)}\left(1 + \dfrac{T_0\Delta_i/(1+\Delta_i)}{T_m - T_0 + \eta_{21}}\right) - 1 & (T = T_0; K_j \neq \infty), \\ 0 & (T = T_0; K_j = \infty), \end{cases}$$

$$\gamma_{ij} = N_i/N_j = \tau c_i/K_j \leqslant 1. \quad (3)$$

The same approach applies to the extensibility. The γ_{ij} is the volume or number ratio between the ith surface atomic layer of thickness d_i and the entire nanostructure of size K_j, K_j being the dimensionless form of size is the number of atoms lined along the radius of a spherical dot or cross the thickness of a thin slab. Equation (3) represents that the undercoordinated atoms in the surface skin dictates the relative change of mechanical properties, yet atoms in the interior remain their bulk features. Compared with the analytical expression for the inverse Hall-Petch relationship,[43] the current form in Eq. (3) represents the intrinsic change of modulus or strength excluding the effect of dislocation accumulation and the artifacts due to indentation tip shapes, strain rates, loading scales, etc., involved in the indentation test.[44]

C. Debye temperature

The Debye temperature, which is defined as $\theta_D = \hbar\omega_D/k_B$ in the Debye model of the specific heat, is a key parameter that determines the thermal transport dynamics properties. When the solid size is reduced or the temperature of measurements is varied, θ_D is no longer constant but change depending on the object size[45–48] and testing temperature.[49–52] Calculation results[45] suggested that the size dependence of θ_D results from the finite cutoff of frequency and surface stresses (effectively form a size-dependent change of surface pressure), especially if the size is smaller than 20 nm. Using x-ray-absorption spectra measurements and extended x-ray-absorption fine-structure spectroscopy, Balerna and Mobilio[46] confirmed the predicted trend.[45] The temperature-dependent θ_D was another interesting observation. Calculations of the temperature-dependent θ_D of some fcc and bcc metals[49] revealed that the θ_D decreased when the temperature was increased due to the temperature dependence of elastic constants and sound velocity of the solid. However, a discrepancy remains regarding the T_m dependence of the T-independent θ_D. One opinion is that the θ_D varies linearly with the T_m (Ref. 49), and the other suggests a square-root dependence on T_m according to Lindemann's[53] criterion of melting.

The Debye temperature θ_D can be derived from the mathematical expression for the normalization of phonon density states: $\int_0^{\omega_D} g(\omega)d\omega = \kappa N_A$, with N_A being the total number of vibration modes, giving rise to the relation $\omega_D \propto v_s(n)^{1/\kappa} \propto v_s(d^{-\kappa})^{1/\kappa} = v_s/d$, where $v_s = \sqrt{Y/\rho} \sim \sqrt{Yd^3}$ is the sound velocity in the medium and κ is the fractal dimensions ($\kappa = 1$

for nanowires, $\kappa=2$ for thin plates, and $\kappa=3$ for bulk material). Because the Debye temperature is defined as $\theta_D=\hbar\omega_D/k_B$, the normalized expression for θ_D has the following form:

$$\frac{\theta_D(z_i,m,T)}{\theta_D(z_b,m,T_0)}=\frac{\omega_D(z_i,m,T)}{\omega_D(z_b,m,T_0)}=\frac{v_s(z_i,m,T)}{v_s(z_b,m,T_0)}\cdot\frac{d_0}{d_i}=\left(c_i\frac{Y(z_i,m,T)}{Y(z_b,m,T_0)}\right)^{1/2}. \tag{4}$$

Combining Eqs (1) and (4) leads to immediate relation

$$\frac{\Delta\theta_D(K_j,m,T)}{\theta_D(\infty,m,T_0)}=\sum_{i\leqslant 3}\frac{\tau c_i}{K_j}\left\{c_i^{-(1+m/2)}\left[\frac{T_m-T/(1+\Delta_i)}{T_m-T_0+\eta_{21}}\right]^{1/2}-1\right\}=\sum_{i\leqslant 3}\frac{\tau c_i}{K_j}\left\{c_i^{-(1+m/2)}\left[1+\frac{T_0-T/(1+\Delta_i)}{T_m-T_0+\eta_{21}}\right]^{1/2}-1\right\}. \tag{5}$$

Therefore, the current form [Eq. (5)] has a square-root dependence on $(T_m-T)^{1/2}$ for the bulk ($\Delta_i=0$, $c_i=1$, if the surface effect is ignored), being different from the linear[49] or square-root dependence on T_m: $\theta_D\propto T_m^{1/2}/d$ (Ref. 53).

D. Specific heat capacity

The specific heat capacity is a measurable physical quantity that characterizes the ability of a body to store the heat when the sample temperature is changed. The effect of body size on the specific heat capacity has recently attracted a lot of attention.[54–57] Novotny *et al.*[54] measured the low-temperature heat capacity of 2.2- and 3.7-nm-sized lead particles and observed the enhancement of heat capacity below 5 K. Lu[58] demonstrated that the specific heat of metallic or alloying nanosolids increases with the inverse of solid size. An ac microcalorimeter measurement[55] shown that the specific heat of Al thin films with film thickness varying from 13.5 to 370 nm reduces with the thickness of the Al film. The decrease of specific heat was explained by the rise of the absorption and the loss of thermal waves with specific wave vectors in the small volumes. However, Lu *et al.*[56] calculated the size effects on the specific heat of Al thin film employing the Prasher-Phetan[59] approach and derived that the reduction of phonon states was not the main reason causing the size effect on specific heat, but a thin layer of Al oxide was responsible for it. In the measurement of Yu *et al.*,[57] the heat capacity decreased with the film thickness; however, the specific heat increased as the film become thinner, in disagreement with the measured results of Song *et al.*[55] Therefore, the discrepancies in the role of the size and temperature dependence of the heat capacity and Debye temperature for metallic nanostructures remain unsolved.

The heat capacity per unit volume is defined as the ratio of an infinitely small amount of heat δE added to the body to the corresponding small increase in its temperature δT when the volume is kept unchanged. In the extended Debye model the expression is given by

$$C_v=\left(\frac{\partial E}{\partial T}\right)_V=\kappa^2R\left(\frac{T}{\theta_D}\right)^{\kappa}\int_0^{\theta_D/T}\frac{x^{\kappa+1}\exp(x)}{[\exp(x)-1]^2}dx, \tag{6}$$

where $x=\hbar\omega/k_BT$. It can be shown that when $\kappa=3$, Eq. (6) is reduced to the standard expression in the three-dimensional Debye model. In the case of $T\gg\theta_D$, the integration in Eq. (6) gives $(1/\kappa)(\theta_D/T)^{\kappa}$. The heat capacity C_v is substituted by κR, in agreement with the Dulong-Petit law in the case of $\kappa=3$. C_v approaches a constant value at high temperatures. The low-temperature limit of the heat capacity is even more interesting. If $T\ll\theta_D$, the upper limit of the integral of Eq. (6) approaches infinity and the integration gives $\int_0^{\infty}x^{\kappa+1}e^x/(e^x-1)^2dx\approx 3.290$, 7.212, and 25.976, for $\kappa=1$, 2, and 3. Therefore, the heat capacity in the low-temperature limit becomes

$$C_v=A\kappa^2\left(\frac{T}{\theta_D}\right)^{\kappa}\propto\kappa^2\theta_D^{-\kappa}, \tag{7}$$

where A is a fixed value for a given τ. From Eqs. (6) and (7), we can see that the Debye temperature θ_D has a strong effect on the heat capacity. Using the same core-shell structure, we can obtain the expression for heat capacity per unit volume depending on the size, shape, and bond nature at very low temperatures ($T\sim 0$):

$$\frac{\Delta C_v(m,T,K_j)}{C_v(m\,.\,T_0,\infty)}=\sum_{i\leqslant 3}\frac{\tau c_i}{K_j}\left[c_i^{(1+m/2)\kappa}\left(\frac{1-T/T_m(1+\Delta_i)}{1-T_0/T_m}\right)^{-\kappa/2}-1\right]\cong\sum_{i\leqslant 3}\frac{\tau c_i}{K_j}[c_i^{(1+m/2)\kappa}(1-T_0/T_m)^{\kappa/2}-1]<0\quad(T\sim 0). \tag{8}$$

Since the coefficient of bond contraction c_i is always smaller than unity, the heat capacity is always lower than the bulk value at the lower temperatures and the heat capacity decreases inversely with the solid size (K_j). At temperature close to the Debye temperature, the heat capacity should be evaluated using Eq. (6), where the Debye temperature is size, temperature, and bond nature dependent according to Eq. (5).

III. RESULTS AND DISCUSSION

Using Eq. (3), we are able to predict the bond nature, solid shape and size, and the $x_m(T/T_m)$ dependence of the Young's modulus and extensibility of a solid. For illustration purposes, we selected $m=1$ (for metals), 3 (carbon, 2.56), and 5 (Si, 4.88), $x_m=0.25$, 0.5, and 0.75, and the dimensionality $\tau=3$ (for a sphere) to conduct the calculations. The T_0 was set at 0 K and T, respectively. For temperature dependence, we used $K_j=10$ and 50 sizes by fixing other parameters. η_{21} was taken as zero for illustration purposes; otherwise, a small offset could hardly be identified in the predicted relative changes.

Figure 1(a) shows that elevation or depression of the Young's modulus with decreasing sizes may happen depend-

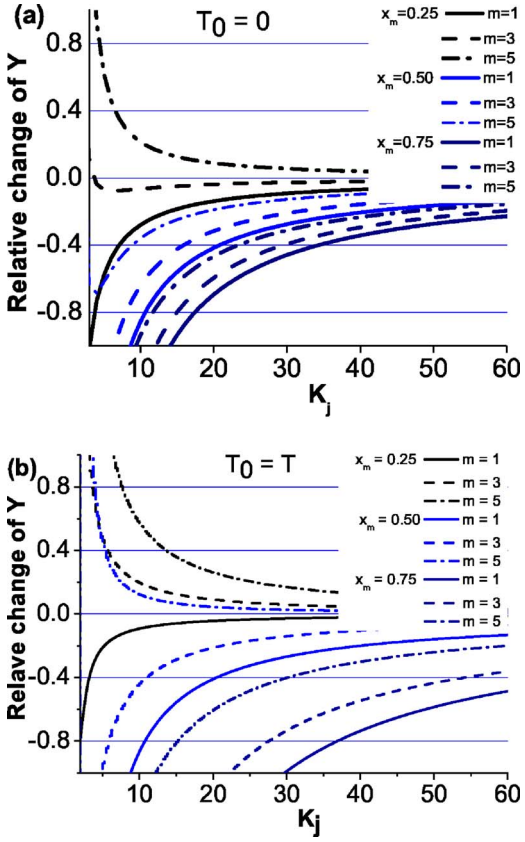

FIG. 1. (Color online) Prediction of size K_j dependence of Young's modulus with (a) $T_0=0$ and (b) $T_0=T$ of different bond nature and x_m (T/T_m) values. Young's modulus enhancement happens at the combinations of $(x_m,m)=(<0.25,>3)$ for $T_0=0$ and $(x_m,m)=(<0.5,>3)$ for $T_0=T$. The Y retention may happen at critical $(T/T_m,m)$ combinations.

ing on the combination of (x_m,m) values. For example, Y elevation occurs in the situations of $(x_m,m)=(<0.25,>3)$. Y retention may happen at critical (x_m,m) combinations such as $(x_m,m)=(\sim 0.25,\sim 3)$. The critical combination of (x_m,m) can be obtained by approaching Eq. (3) to zero. If we select $T=T_0$, Y elevation also occurs in the situations of $(x_m,m)=(<0.5,>5)$. The Y may also remain constant at $(x_m,m)=(0.25,\sim 2)$ and $(0.5,\sim 4)$. It is not surprising therefore that the modulus may rise, drop, or remain constant upon the solid size being reduced, depending on the materials and operating conditions, and techniques as well.

Figure 2 shows the temperature-induced relative change of (a) Y values and (b) the extensibility for $K_j=10$ and $m=1,3,5$ samples. If $T_0=T$, the Y drops nonlinearly with T until T_m. The insertion shows the case of $T_0=0$ in which the Y drops linearly with T. The extensibility approaches infinity at the corresponding $T_m(K_j)$. The inset manifests singularities because of the shell-by-shell configuration. If we treat the outermost two atomic layers as the skin with a mean $z_i=(4+6)/2$ and the singularity occurs at the melting point, the extensibility drops with the characteristic dimension. On the other hand, a smaller nanosolid with lower m value is more easily extensible at elevated temperatures than the other cases.

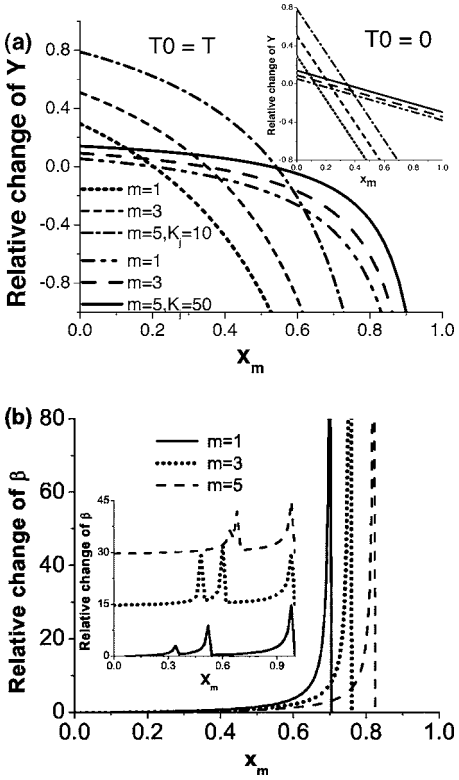

FIG. 2. T/T_m dependence of (a) Young's modulus and (b) extensibility of a spherical nanosolid with different m and T/T_m (x_m) ratios. The insertion shows the cases of $T_0=0$. The Y values of nanosolid of lower m values and smaller sizes drop faster when the test temperature is raised. The extensibility approaches infinity at the melting point. The singularities in the inset exhibit the shell-by-shell melting features.

Figure 3 compares the prediction with observations of the size dependence of the Y values for (a) ZnO and (b) polymers measured at room temperature and temperature-dependent Y value for (c) bulk Al_2O_3 and (d) bulk AlN. Predictions agree exceedingly well with the measured data for ZnO nanowires ($m=4$, $\tau=2$). For the polymer, predictions agree with the general trend of measurement [$m=4$, $\tau=1$ (film)] with accuracy subject to the precision of the size determination. Numerical agreement of the temperature dependence of the Y [Fig. 3(c)] at higher temperatures could be made by the discussed models despite the physical mechanisms. However, we found that the $B=[E_b(0)\times(1+\alpha T)^3]^{-1}$ in Anderson's and the T_0 in Wachtman's correspond to the turning point T_0 at which the T-Y curve transits from nonlinear to linear, which is governed by the Debye temperature. Besides, our approach covers the contribution from thermal expansion. The overall performance of the BOLS prediction may represent the true situation of thermally softened specimens.

The predicted m, K_j, and x_m dependence of the modulus and extensibility covers all the possible trends as observed. For example, the predicted Y depression in Fig. 1 agrees well with the measured trends of Al [$m=1$, $x_m=300/650\sim 0.5$ (Ref. 22)] and polymers [$T_g=300/450\sim 2/3$ (Ref. 24)]. The extensibility of nanoscaled Al-Cu alloys in the semisolid state,[36] and nanoscaled Al_2O_3 (Ref. 60) and PbS (Ref. 61) at

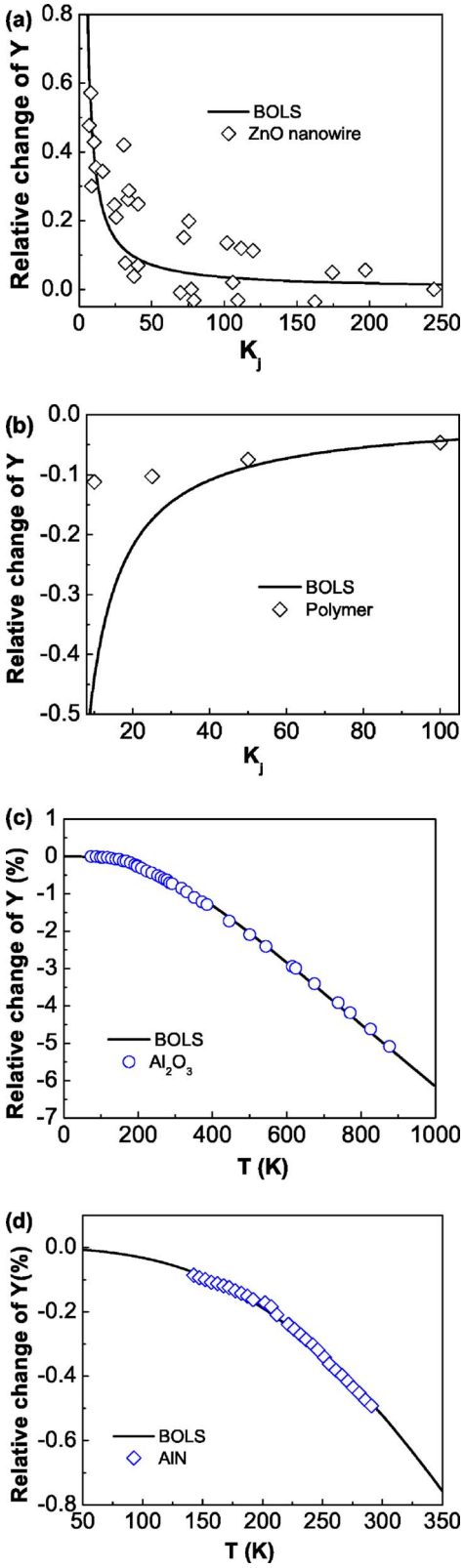

FIG. 3. (Color online) Matching predictions to the measurement of Y value (a) enhancement of ZnO nanowires (Ref. 8), (b) suppression of polymer (Ref. 14) and the temperature dependence of the Y values for (a) AlN (T_m=3273 K, θ_D=1150 K, E_B=5.19 eV) (Ref. 21) and (b) Al_2O_3 (T_m=2303 K, θ_D=1045 K, E_B=3.9 eV) (Ref. 39), with T_m and θ_D as input and E_B (the atomic cohesive energy in the bulk at 0 K) as output.

room temperature increases generally with grain refinement. The m values for compounds or alloys are around 4 or higher, and their T/T_m ratios are relatively lower. The increase of the compressibility and extensibility of Al_2O_3 and PbS nanosolids renders Young's modulus. The superplasticity of materials such as Cu wires [m=1, $x_m \sim 1/2$ (Ref. 62)] with grain size less than tens of nanometers in the temperature range 0.5–0.6 T_m (Ref. 63) also agrees with the predictions. The Y elevation of ZnO nanowire [m=4, $x_m \sim 1/4$ (Ref. 8)] and Si nanosphere [m=4.88, $x_m \sim 1/6$ (Ref. 2)] is also within the prediction because of their high m values and low x_m ratios. However, the discrepancy of ZnO wires[8–11] and Si spheres[2] and belts[16] may arise from different x_m of operation or different experimental conditions or methods. It is anticipated that modulus enhancement as observed from TiCrN and GaAlN surfaces[6] may not be observable at room temperature for the low-T_m metals such as Sn, Pb, Al, Zn, Mg, and In.

Predictions also agree with the temperature dependence of Young's modulus of chemical vapor deposition (CVD) nanodiamond films,[23] the silicone resins,[24] and the yield stress (linearly proportional to modulus) of Mg nanosolid[64] of a given size. The ductility increases exponentially with temperature until infinity at T_m that drops with solid size. An atomic-scale simulation[65] also suggests that the material becomes softer in both the plastic and elastic regimes as the operating temperature is raised. When measuring at 200 °C, the strength of 300-nm-sized Cu nanograins is lowered by 15% and the ductility increases substantially.[66] When the operation temperature is increased from room temperature to 400 °C the ductility of ultrafine-grained $FeCo_2V$ samples of 100–290 nm sizes increases from 3–13% to 22% rendering with strength attenuation.[67] The biaxial Young's modulus of Si (111) and Si (100) drops linearly when the T is increased.[68,69] A 280% superplasticity of single-walled carbon nanotube (m=2.56, $x_m \sim 2/3$) has been realized at high temperature.[70]

It is true that the Young's modulus and tensile stress and strength are indeed different quantities despite the similarity in the trends of change with external stimulus as widely observed from specimens such as polymers[71] and Al oxide[4] on the size and temperature dependence. From an atomistic point of view, these quantities are intrinsically related to the bonding energy and bond length and thus we can explain why they perform with similar trends. Artifacts in the measurement, in particular in the plastic deformation regime, may dominate as extrinsic contributions to modulate the slope of measured data. The consistency between observations and predictions of the linear dependence of mechanical properties may provide evidence for the BOLS consideration.

Using Eq. (5), we are able to predict the dependence of θ_D on the size (K_j), temperature (T), and bond nature (m). Figure 4 shows the relative change of θ_D for nanowires (τ=2, κ=1) with m=1,3,5 and x_m=0, 0.25, and 0.50. When the temperature of the measurement is much lower than the melting point ($x_m \ll 1$), θ_D increases with the decrease of material dimension K_j, while θ_D increases faster at larger m. On the other hand, θ_D decreases with increasing operation tem-

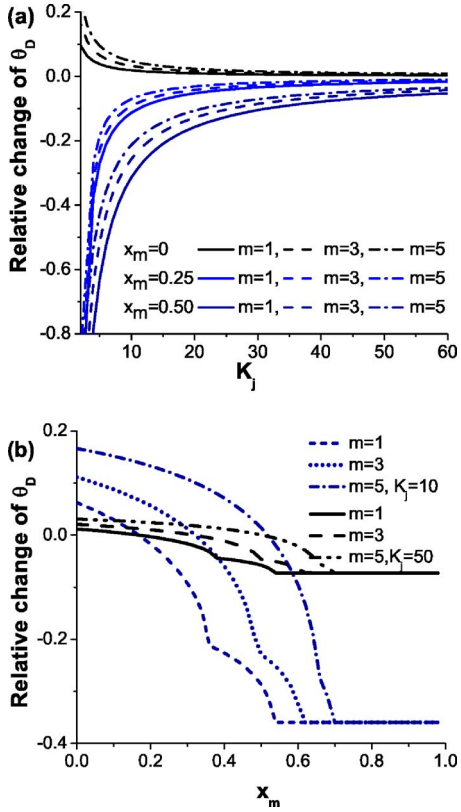

FIG. 4. (Color online) Prediction of (a) size (K_j) and (b) temperature x_m (T/T_m) dependence of θ_D for different bond nature (m). The θ_D increases with the decreasing of size for very low T and decreases with decreasing the size for high temperature. The θ_D of nanowires with higher m values and smaller size drops faster when the temperature is raised. The transition points correspond to local melting temperature of the outermost two atomic layers.

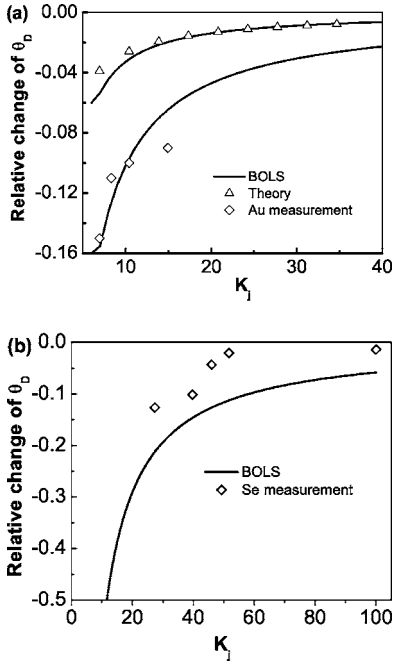

FIG. 5. Comparison of the BOLS predictions with the observations based on (a) Couchman and Karasz's model (with $T_0=0.245T_m$, $T=0.16T_m$, $T_m=1337$ K) (Ref. 45) and measurement (with $T_0=0.224T_m$, $T=0.204T_m$) (Ref. 46) for Au particles and (b) Se particles (with $T_0=T=0.6T_m$, $T_m=494$ K) (Ref. 47).

perature and the relative change of θ_D is greater for smaller m values. A close examination of Fig. 4(a) and Eq. (5) could lead to a conclusion that for a certain (x_m,m) combination, the Debye temperature may vary insignificantly with particle size, being the same as Young's modulus retention. Figure 4(b) shows the temperature-induced relative change of θ_D for nanowires ($\tau=2,\kappa=1$) of size $K_j=10$ and 50. If we set $T_0=T$, the θ_D decreases nonlinearly with temperature T until T approaches T_{mi} (local melting temperature of the ith atomic site). The two transition points for each of the (m,K_j) combinations arise from the loss of bond that happens only to the outermost two discrete atomic layers. Moreover, the variation of θ_D with the temperature and size is more pronounced for larger m and smaller K_j values.

Figure 5 compares the predictions with various theoretical or experimental data (a) for Au particles and (b) Debye temperature from Debye-Waller parameter measurements for Se nanoclusters. Couchman and Karasz's approach[45] shows that the change of Debye temperature involves the particle size R and cutoff acoustic wave vectors K_0: $\Delta\theta_D/\theta_0 \approx -3\pi/8RK_0$, without temperature being involved. By applying Eq. (5), with $T_0=0.245T_m$ and $T=0.16T_m$, agreement between the BOLS prediction and Couchman and Karasz's estimation has been reached. If we set $T_0=0.224T_m$ and $T=0.204T_m$, our model fits Balerna and Mobilio's measurement results quite well, which is also shown in Fig. 5(a). In Fig. 5(b), the prediction shows the general trend of the Debye temperature with respect to size; agreement is not satisfied. However, the measurement was conducted at $T=293$ K, which is higher than the local melting temperature of the first two layers, about $0.6T_m$ (for Se $T_m=494$ K), and hence the giving feature is dominated by a core interior with less temperature dependence.

As indicated in Eq. (6), the specific heat capacity depends unambiguously on the θ_D and hence on the size, temperature, and bond nature. Figure 6(a) shows the reduced C_v (in units of R, where R is a gas constant) versus temperature (T/θ_{D0}) for Si nanowires ($m=4.88$) and Al nanowires ($m=1$) of different diameters ($K_j=5$, 10, and 20). The shape of the C_v curve is similar to that of the bulk C_v curve of the Debye model, but with the size-induced depression over the whole temperature range. For the same K_j at the given T/θ_{D0}, the reduction of heat capacity is larger for larger m. Figure 6(b) plots C_v/C_{v0} (where C_{v0} is the bulk heat capacity at a given temperature) vs K_j at $T=100$ and 300 K for Al nanowires and Si nanowires. The heat capacity decreases with the size at fixed temperature (except for Al nanowires measured at room temperature, such that the heat capacity is very close to the bulk C_v value obtained when $K_j>15$ and increases slightly with decreasing size). For a given size, the reduction of the heat capacity is more significant at lower temperatures or larger m value. In this analysis, we set $T_0=T$. If T_0 is assumed to be 0, the general trend of the heat capacity is preserved, but the reduction of the heat capacity is greater.

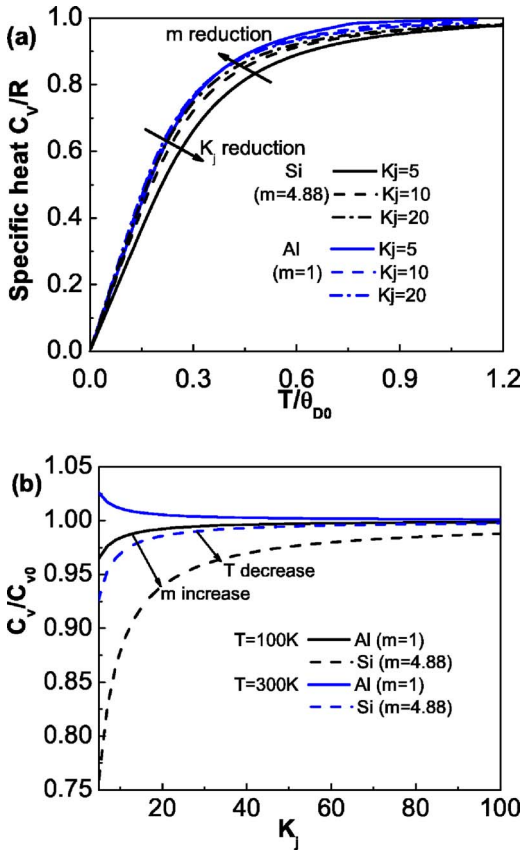

FIG. 6. (Color online) (a) Temperature (T/θ_{D0}) and size dependence of heat capacity (in units of R) for Si nanowires (m=4.88) and Al nanowires (m=1) with K_j=5, 10, and 20 and T=100 K and 300 K, in panels (a) and (b). The heat capacity approaches R at very high temperature, and decreases with decreasing size. The reduction of the heat capacity is more pronounced for larger m values at a given T/θ_{D0}. The heat capacity generally reduces with solid size and reduces faster at lower temperature and larger m values.

IV. CONCLUSION

A set of analytical expressions for the size, temperature, and bond nature dependence of the elastic modulus and its derivatives on the extensibility, Debye temperature, and specific heat of nanostructures has been established in terms of bonding identities and their coordination and temperature dependence, which covers the essential parameters and their interdependence. Understanding clarifies why the Y values for some materials are elevated and why those of others are not upon size reduction and how the mechanical strength drops when the measuring temperature is increased. Conclusions can be drawn as follows.

(a) The Young's modulus of a nanosolid may depress, increase, or remain unchanged, depending on the size, temperature of operation, and the nature of bond involved, as well as experimental conditions. It is therefore not surprising to observe the elastic modulus change in different trends of different materials measured under different conditions. It is suggested that one could not consider a certain parameter at a time without addressing the rest when discussing the mechanical and thermal properties of a material, especially a small object.

(b) The similarity of the size and temperature dependence of the mechanical properties such as Young's modulus, tensile stress and strength, and surface energy arises intrinsically from the same origin of bonding energy and bond length. Artifacts in measurements, in particular in the plastic regime, may dominate as extrinsic contributions to modulate the observations extrinsically.

(c) Agreement between observations and predictions of the T-dependent Young's modulus has allowed us to derive information about the bonding energy of an atom in the bulk, which goes beyond conventional theoretical and experimental approaches.

(d) The θ_D has a square-root dependence on $(T_m - T)$, rather than a linear or square-root dependence on the T_m. The currently derived solution may provide complementary information for the T-independent form of θ_D given by Lindemann.

(e) The specific heat capacity generally decreases when the solid size is reduced. The reduction of the specific heat capacity is more pronounced for larger m values at lower temperatures.

(f) Further exploration of the temperature dependence of Y, β, θ_D, and C_v at extremely low temperature would be even more interesting and an investigation is in progress.

*Electronic address: ecqsun@ntu.edu.sg; URL: http://www.ntu.edu.sg/home/ecqsun/

[1] R. Dingreville, J. M. Qu, and M. Cherkaoui, J. Mech. Phys. Solids **53**, 1827 (2005).
[2] W. W. Gerberich, W. M. Mook, C. R. Perrey, C. B. Carter, M. I. Baskes, R. Mukherjee, A. Gidwani, J. Heberlein, P. H. McMurry, and S. L. Girshick, J. Mech. Phys. Solids **51**, 979 (2003).
[3] G. Y. Jing, H. L. Duan, X. M. Sun, Z. S. Zhang, J. Xu, Y. D. Li, J. X. Wang, and D. P. Yu, Phys. Rev. B **73**, 235409 (2006).
[4] J. Q. Broughton, C. A. Meli, P. Vashishta, and R. K. Kalia, Phys. Rev. B **56**, 611 (1997).
[5] G. Y. Jing, H. Ji, W. Y. Yang, J. Xu, and D. P. Yu, Appl. Phys. A: Mater. Sci. Process. **82**, 475 (2006).
[6] C. Q. Sun *et al.*, J. Appl. Phys. **90**, 2615 (2001).
[7] R. E. Miller and V. B. Shenoy, Nanotechnology **11**, 139 (2000).
[8] C. Q. Chen, Y. Shi, Y. S. Zhang, J. Zhu, and Y. J. Yan, Phys. Rev. Lett. **96**, 075505 (2006).
[9] A. J. Kulkarni, M. Zhou, and F. J. Ke, Nanotechnology **16**, 2749 (2005).
[10] J. Song, X. Wang, E. Riedo, and Z. L. Wang, Nano Lett. **5**, 1954 (2005).
[11] X. D. Bai, P. X. Gao, Z. L. Wang, and E. G. Wang, Appl. Phys. Lett. **82**, 4806 (2003).
[12] K. Yum, Z. Wang, A. P. Suryavanshi, and M. F. Yu, J. Appl. Phys. **96**, 3933 (2004).

[13] M. Kopycinska-Muller, R. H. Geiss, J. Muller, and D. C. Hurley, Nanotechnology **16**, 703 (2005).
[14] W. J. Price, S. A. Leigh, S. M. Hsu, T. E. Patten, and G. Y. Liu, J. Phys. Chem. A **110**, 1382 (2006).
[15] S. G. Nilsson, X. Borrise, and L. Montelius, Appl. Phys. Lett. **85**, 3555 (2004).
[16] X. Li, T. Ono, Y. Wang, and M. Esashi, Appl. Phys. Lett. **83**, 3081 (2003).
[17] X. Li, X. Wang, Q. Xiong, and P. C. Eklund, Nano Lett. **5**, 1982 (2005).
[18] C. Gaire, D. X. Ye, F. Tang, R. C. Picu, G. C. Wang, and T. M. Lu, J. Nanosci. Nanotechnol. **5**, 1893 (2005).
[19] B. Wu, A. Heidelberg, and J. J. Boland, Nat. Mater. **4**, 525 (2005).
[20] B. Wu, A. Heidelberg, J. J. Boland, J. E. Sader, X. Sun, and Y. Li, Nano Lett. **6**, 468 (2006).
[21] S. P. Dodd, G. A. Saunders, M. Cankurtaran, and B. James, J. Mater. Sci. **36**, 723 (2001).
[22] M. A. Haque and M. T. A. Saif, Thin Solid Films **484**, 364 (2005).
[23] F. Szuecs, M. Werner, R. S. Sussmann, C. S. J. Pickles, and H. J. Fecht, J. Appl. Phys. **86**, 6010 (1999).
[24] Y. H. Wu, F. J. McGarry, B. Z. Zhu, J. R. Keryk, and D. E. Katsoulis, Polym. Eng. Sci. **45**, 1522 (2005).
[25] H. Liang, M. Upmanyu, and H. Huang, Phys. Rev. B **71**, 241403(R) (2005).
[26] H. W. Shim *et al.*, Appl. Phys. Lett. **86**, 151912 (2005).
[27] S. Cuenot, C. Fretigny, S. Demoustier-Champagne, and B. Nysten, Phys. Rev. B **69**, 165410 (2004).
[28] V. B. Shenoy, Phys. Rev. B **71**, 094104 (2005).
[29] J. G. Guo and Y. P. Zhao, J. Appl. Phys. **98**, 074306 (2005).
[30] H. A. Wu, Mech. Res. Commun. **33**, 9 (2006).
[31] C. Q. Sun, Y. Shi, C. M. Li, S. Li, and T. C. Au Yeung, Phys. Rev. B **73**, 075408 (2006).
[32] C. Q. Sun, L. K. Pan, C. M. Li, and S. Li, Phys. Rev. B **72**, 134301 (2005).
[33] C. Q. Sun, Prog. Solid State Chem. **35**, 1 (2007).
[34] C. Q. Sun, C. M. Li, S. Li, and B. K. Tay, Phys. Rev. B **69**, 245402 (2004).
[35] M. Born, J. Chem. Phys. **7**, 591 (1939).
[36] D. G. Eskin, Suyitno, and L. Katgerman, Prog. Mater. Sci. **49**, 629 (2004).
[37] J. Campbell, *Castings* (Butterworth-Heinemann, Oxford 1991).
[38] U. Gysin, S. Rast, P. Ruff, E. Meyer, D. W. Lee, P. Vettiger, and C. Gerber, Phys. Rev. B **69**, 045403 (2004).
[39] J. B. Wachtman, W. E. Tefft, Jr., and D. G. Lam, Phys. Rev. **122**, 1754 (1961).
[40] R. J. Bruls, H. T. Hintzen, G. de With, and R. Metselaar, J. Eur. Ceram. Soc. **21**, 263 (2001).
[41] O. L. Anderson, Phys. Rev. **144**, 553 (1966).
[42] The z_i for the outermost atomic layer changes with the surface curvature or the dimensionality of the nanostructure (for spherical dot, $\tau=3$, for a cylindrical rod, $\tau=2$) in the form of $z_1=4\times(1-0.75/K_j)$. For a flat surface ($\tau=1$), $z_1=4$. Generally, $z_2=6$ and $z_i>3=12$.
[43] The relative specific heat satisfies that inverse Hall-Petch relation $\eta_1(K_j)/\eta_1(\infty)=1+AK_j^{-0.5}$, which includes the effect of dislocation accumulation.
[44] V. Brazhkin, N. Dubrovinskaia, M. Nicol, N. Novikov, R. Riedel, V. Solozhenko, and Y. Zhao, Nat. Mater. **3**, 576 (2004).
[45] P. R. Couchman and F. E. Karasz, Phys. Lett. **62A**, 59 (1977).
[46] A. Balerna and S. Mobilio, Phys. Rev. B **34**, 2293 (1986).
[47] Y. H. Zhao and K. Lu, Phys. Rev. B **56**, 14330 (1997).
[48] C. C. Yang, M. X. Xiao, W. Li, and Q. Jiang, Solid State Commun. **139**, 148 (2006).
[49] M. Blackman, Proc. R. Soc. London, Ser. A **148**, 365 (1935).
[50] R. C. G. Killean and E. J. Lisher, J. Phys. C **8**, 3510 (1975).
[51] S. Peng and G. Grimvall, J. Phys. Chem. Solids **55**, 707 (1994).
[52] C. J. Martin and D. A. O'Connor, J. Phys. C **10**, 3521 (1977).
[53] F. A. Lindemann, Phys. Z. **11**, 609 (1910).
[54] V. Novotny, P. P. M. Meincke, and J. H. P. Watson, Phys. Rev. Lett. **28**, 901 (1972).
[55] Q. Song, C. Zheng, S. Xia, and S. Chen, Microelectron. J. **35**, 817 (2004).
[56] Y. Lu, Q. L. Song, and S. H. Xia, Chin. Phys. Lett. **22**, 2346 (2005).
[57] J. Yu, Z. A. Tan, F. T. Zhang, G. F. Wei, and L. D. Wang, Chin. Phys. Lett. **22**, 2429 (2005).
[58] K. Lu, Mater. Sci. Eng., R. **16**, 161 (1996).
[59] R. S. Prasher and P. E. Phelan, Int. J. Heat Mass Transfer **42**, 1991 (1999).
[60] B. Chen, D. Penwell, L. R. Benedetti, R. Jeanloz, and M. B. Kruger, Phys. Rev. B **66**, 144101 (2002).
[61] S. B. Qadri, J. Yang, B. R. Ratna, E. F. Skelton, and J. Z. Hu, Appl. Phys. Lett. **69**, 2205 (1996).
[62] L. Lu, M. L. Sui, and K. Lu, Science **287**, 1463 (2000).
[63] K. S. Siow, A. A. O. Tay, and P. Oruganti, Mater. Sci. Technol. **20**, 285 (2004).
[64] N. Ono, R. Nowak and S. Miura, Mater. Lett. **58**, 39 (2004).
[65] J. Schiotz, T. Vegge, F. D. Di Tolla, and K. W. Jacobsen, Phys. Rev. B **60**, 11971 (1999).
[66] N. A. Krasilnikov, Z. Pakiela, W. Lojkowski, and R. Z. Valiev, Solid State Phenom. **94**, 51 (2003).
[67] A. Duckham, D. Z. Zhang, D. Liang, V. Luzin, R. C. Cammarata, R. L. Leheny, C. L. Chien, and T. P. Weihs, Acta Mater. **51**, 4083 (2003).
[68] P. Kury and M. Horn-von, Rev. Sci. Instrum. **75**, 1357 (2004).
[69] Y. A. Burenkov and S. P. Nikanorov Sov. Phys. Solid State **16**, 963 (1974).
[70] J. Y. Huang, S. Chen, Z. Q. Wang, K. Kempa, Y. M. Wang, S. H. Jo, G. Chen, M. S. Dresselhaus, and Z. F. Ren, Nature (London) **439**, 281 (2006).
[71] J. F. de Deus, A. C. Tavares, C. M. Lepienski, and L. Akcelrud, Surf. Coat. Technol. **201**, 3615 (2006).